

reactance using this simple geometrical approach yield agreement with experiment for high electron densities. Further studies are being made of the behavior of electrode parameters at lower values of (P/V), where variations in the experimental values are not explained by the assumed models.

These considerations show that the electrode effects may be neglected and indicate that the elementary theory of the positive column may be used to relate the externally measured power and voltage to the plasma parameters. Measurements have been made which indicate that this model may be used over a range of pR from 0.4 to 0.8 Torr-cm. Confirmation of the linear dependence of average electron density on P/V and that the electron energy distribution function is independent of P/V was obtained by measuring the intensity of the neon $5s_2 \rightarrow 2p_2$ emission line at 4928 Å. It is expected that the population of the $5s_2$ energy state is predominantly due to single electron collisions; consequently, the emission line intensity should be proportional to electron density if the electron energy distribution is constant.³ The measured intensity was proportional to P/V for values of $P/V > 75$.

Further experimental measurements were made in which the electrical parameters were measured for two lengths of discharge column with otherwise identical electrode geometry. Direct subtraction then provides a measure of power density and voltage per unit length of positive column. These measurements were made on a 0.75-cm-radius discharge tube at a pressure of 1.1 Torr in a 90% helium 10% neon gas mixture. Using the mean collision frequency computed for the electron temperature taken from the data of Bekefi and Brown⁷ for pure helium and the measured values for P_{ec} and E_0 , the average electron density obtained as a function of P/V is shown plotted in Fig. 1. These measurements showed E_0 to be independent of P/V in further confirmation of the invariance of ϵ_0 over the ranges measured.

* This work is supported by the Bureau of Naval Weapons, U. S., Department of the Navy, under Contract NOW 62-0604-c.
¹ E. F. Labuda and E. I. Gordon, *J. Appl. Phys.* **35**, 1647 (1964).
² A. von Engel, *Ionized Gases* (Clarendon Press, Oxford, 1955), Chap. 8.
³ A. D. White and E. I. Gordon, *Appl. Phys. Letters* **3**, 197 (1963).
⁴ Gordon Francis, *Ionization Phenomena in Gases* (Butterworths Scientific Publications Ltd., London, 1960).
⁵ J. T. Massey, *J. Appl. Phys.* **36**, 373 (1965).
⁶ The reactance of the positive column is negligible since ν_m is very much greater than the frequency of the source.
⁷ G. Bekefi and Sanborn C. Brown, *J. Appl. Phys.* **32**, 25 (1961).

Hall Effect in Photoconducting Mercuric Sulfide

CONSTANZA VEROLINI AND HOWARD DIAMOND
 University of Michigan, Ann Arbor, Michigan
 (Received 7 October 1964)

THE following describes a method of measuring carrier mobilities via the Hall effect in high-resistivity substances which may also be photoconductors. We utilize this technique here for the measurement of electron mobility in natural cinnabar.

Cinnabar in its pure form has a fairly high dark resistivity (of the order $10^{11} \Omega\text{-cm}$). The measurement of Hall voltage in high-resistivity materials poses a considerable problem in practice. We have been able to obtain a measurable Hall voltage and hence an estimate of carrier mobility by exploiting the natural photoconductivity of cinnabar. In making such a measurement, we illuminate the crystal (held at a constant temperature) with light from a tungsten source. This produces photoexcited carriers (electrons and holes). If the photoconductivity were predominantly of one type (n or p type), then the sign of the Hall voltage would reflect the sign of the predominant charge carrier. The use of photoexcited carriers to obtain mobilities is a valid procedure provided that the recombination time is long compared to the relaxation time. The deduced mobility would be that for the one type of carrier in the crystal if the photoexcited carriers were predominantly of one type. Indications are that the HgS natural crystals used are definitely n -type photoconductors and on the

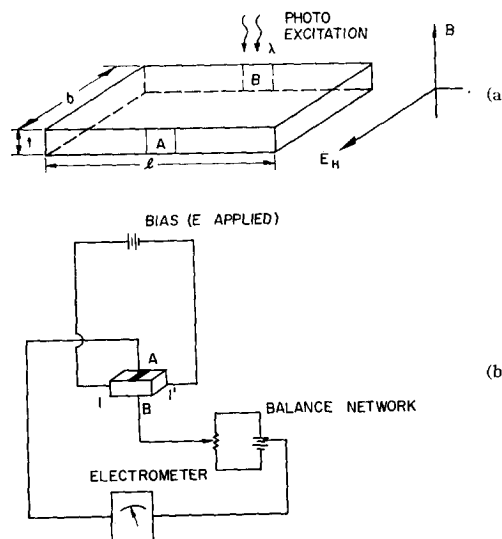


FIG. 1. (a) Crystal configuration with respect to applied fields. A and B are electrodes across which E_H is measured. (b) Bias and electrometer configuration for Hall-voltage measurement.

basis of photoconductive decay experiments we find that the carrier lifetime is well in excess of the transit time (i.e., by several orders of magnitude).

Experimental procedure and results. A natural crystal as shown in Fig. 1(a) was placed in a magnetic field whose axis is in the plane of the paper in the figure. An electrometer connected to electrodes A and B, as shown in Fig. 1(b) measured the Hall field resulting from the action of the magnetic field on the carriers. The density of carriers was increased via photoexcitation by uniform illumination from a tungsten source (about 30 ft-c at sample surfaces). Hence we measure the mobility of the photoexcited carriers. The illumination reduced the resistivity of the samples to a value of about $2 \times 10^8 \Omega\text{-cm}$. The measured parameters for three typical crystals are summarized in Table I.

Crystals A and B were Mexican cinnabar, and crystal C was Alaskan cinnabar. Crystals A and B were polished to cross sections of 1×2 mm and are 3 mm in length. Crystal C has a cross section of 0.5 by 1 mm and is 2 mm long. The contacts on the samples were made by ultrasonic soldering with indium and tested for rectification at the contacts. In all three cases the contacts were found to be Ohmic.

In the following we have assumed electrons to be the majority carrier since the measured Hall field changed polarity whenever the magnetic field was reversed and the Hall coefficient was found to be negative. Photoconductivity decay data also indicate one type of carrier. However, we have not excluded the possibility of considering cinnabar as also having some hole conductivity. For

TABLE I. Measured parameters for three HgS crystals.

A (Mexican cinnabar)	$R = 2 \times 10^8 \Omega$	$B = 0.6 \times 10^{-4} \text{ W/cm}^2$
	$\rho = 1.3 \times 10^8 \Omega\text{-m}$	$t = 1 \text{ mm} = 10^{-3} \text{ m}$
	$I = 10^{-6} \text{ A}$	$l = 3 \times 10^{-3} \text{ m}$
	$E_H = 3 \text{ mV}$	$b = 2 \times 10^{-3} \text{ m}$
	$\mu_n = 39 \text{ cm}^2/\text{V-sec}$	
B (Mexican cinnabar)	$R = 2 \times 10^8 \Omega$	$B = 0.6 \times 10^{-4} \text{ W/cm}^2$
	$\rho = 1.2 \times 10^8 \Omega\text{-m}$	$t = 10^{-3} \text{ m}$
	$I = 10^{-6} \text{ A}$	$l = 3.3 \times 10^{-3} \text{ m}$
	$E_H = 3 \text{ mV}$	$b = 2 \times 10^{-3} \text{ m}$
	$\mu_n = 37 \text{ cm}^2/\text{V-sec}$	
C (Alaskan cinnabar)	$R = 2 \times 10^8 \Omega$	$B = 0.7 \times 10^{-4} \text{ W/cm}^2$
	$\rho = 1 \times 10^8 \Omega\text{-m}$	$t = 0.5 \times 10^{-3} \text{ m}$
	$I = 10^{-6} \text{ A}$	$l = 2 \times 10^{-3} \text{ m}$
	$E_H = 4 \text{ mV}$	$b = 1 \times 10^{-3} \text{ m}$
	$\mu_n = 57 \text{ cm}^2/\text{V-sec}$	

such a case, the computation of mobilities and density of carriers becomes somewhat difficult and an independent method of determining impurity concentrations is required. For the present we proceed with our calculations on a one-carrier basis:

1. *Crystals A and B*: From the data in the above table and from the usual formula

$$\mu = R_H / \rho = E_H t / I B \rho,$$

where R_H = Hall constant, E_H = Hall field (volts), μ = mobility (one carrier), t = thickness (m), I = current through the sample (amperes), B = magnetic field (Wb/m), and ρ = resistivity (Ω -m), we obtain values for mobility of 39 $\text{cm}^2/\text{V}\cdot\text{sec}$ for crystal A, and 37 $\text{cm}^2/\text{V}\cdot\text{sec}$ for crystal B.

2. *Crystal C*: Using the same relations as for samples A and B with the respective values from Table I, the mobility for crystal C is calculated to be 57.1 $\text{cm}^2/\text{V}\cdot\text{sec}$. An estimate for the equilibrium concentration of photoexcited carriers at the given excitation intensity can be given for all three samples. From $R_H = 1/ne$, where $e = 1.6 \times 10^{-19}$ C, n is seen to be of the order of $1.3 \times 10^{18} \text{ cm}^{-3}$.

Wall Deterioration in Flash Lamps

J. H. ROSOLOWSKI AND R. J. CHARLES
General Electric Research Laboratory, Schenectady, New York
(Received 15 December 1964)

A NUMBER of studies of wall deterioration in rare-gas flash lamps under high input power^{1,2} and of tubes containing gas discharges^{3,4} show similar results and thus indicate similar mechanisms of failure. We have analyzed a number of failures of xenon- and neon-filled flash lamps with fused silica walls and our results generally confirm the conclusions of previous investigators.

Failure of flash lamps is preceded by the formation on the inside wall of a loose, milky deposit whose distribution changes with each flash. Hairline cracks, predominantly circumferential, are also observed on the inside wall before total failure. Microscopic examination of broken lamps shows that the cracks pene-

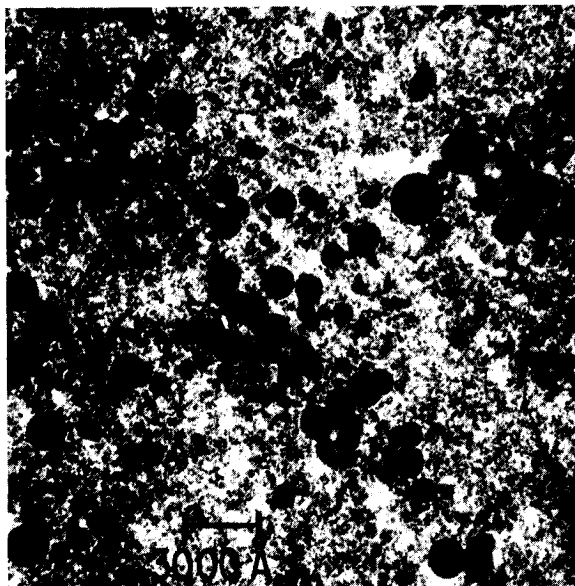


FIG. 1. Electron micrograph of the milky white deposit.

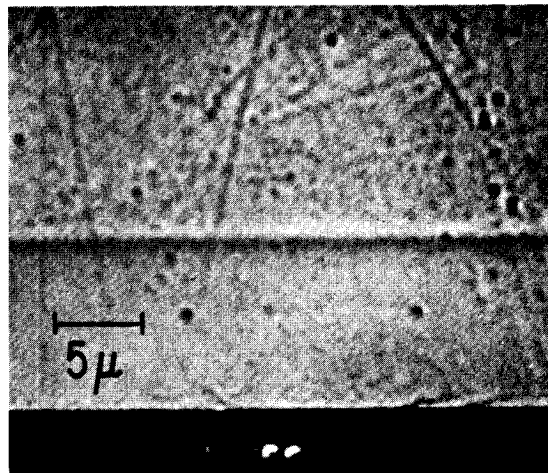


FIG. 2. Electron micrograph of an etched cross section of a lamp which has been flashed with sufficient power to produce the milky deposit, but insufficient to cause rupture.

trate only a short distance. It seems clear that it is these cracks which are responsible for the explosive failure that ultimately occurs on discharging the lamp.

Figure 1 shows an electron micrograph of the milky white deposit. This material, which is undoubtedly an evaporation-condensation product of silica (silica smoke), consists of an appreciable fraction of irregular particles whose characteristic size is about 100 Å and a large number of regular spheres which, in some cases, approach 3000 Å in diameter. Figure 2 is a micrograph of an etched cross section of a lamp which has been flashed with sufficient power to produce the milky deposit but insufficient to cause rupture. It may be noted that the etch (dilute HF acid) preferentially attacked a well-defined layer of the order of 10 μ thick on the inner surface of the tube.

The refractive index was measured by immersing the sample in an oil whose index was known as a function of temperature and observing it with an interference microscope as the oil was heated. The results showed the layer to have a refractive index which was 0.0004 less than that of the silica ($n = 1.4584$) which formed the main body of the tube. This index difference, when analyzed in terms of the Debye formula for refractivity, corresponds to a layer density that is about 0.1% less than that of the rest of the silica. It was also observed that the interference fringes through the layer were somewhat irregular when the layer index was matched to the oil index. This irregularity might be accounted for by some structural inhomogeneity and/or local variations in stress state within the layer.

The fact that the layer index was less than that of normal fused silica excludes the possibility that any significant amount of crystallization occurred. X-ray and electron diffraction patterns taken of the inside and outside of the tubes were also identical and characteristic of amorphous material. It is concluded, therefore, that silica flash lamp failure is not associated with devitrification.

It was further observed that the hairline cracks occur only in the layer, and that immediately upon breaking a lamp they would slowly and spontaneously increase in length. From this one concludes that the layer itself must be in tensile stress.

Table I lists data on four lamps and shows a rough relationship between power input and layer thickness.

These observations support those of Dugdale *et al.*^{3,4} and lead us to conclude that the discharge energy, at peak power, is sufficient to vaporize silica from the inner wall and to melt the glass to an appreciable depth. Calculations using brightness temperatures characteristic for such lamps⁵ and room-temperature optical absorption data for vitreous silica indicate that there is sufficient radiant energy absorption in the first few thousand